

Self-assembly of oligomeric linear dipyrromethene metal complexes†

Qing Miao, Ji-Young Shin, Brian O. Patrick and David Dolphin*

Received (in Berkeley, CA, USA) 17th November 2008, Accepted 16th March 2009

First published as an Advance Article on the web 3rd April 2009

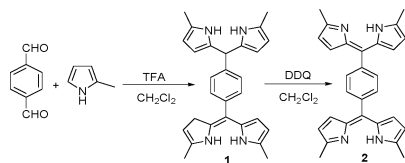
DOI: 10.1039/b820461f

BF₂ capped dipyrin dimers were synthesized and have been used to terminate oligomerization to form a series of controlled length oligomers; the crystal structures of the metal complexes were investigated and correlations between the structures and optical properties were established.

Recently, the study of molecular electronic/photonic wires has become an active platform which involves the use of single or small bundles of molecules as building blocks for energy transportation and electronic applications.^{1,2} In addition, molecular photonics and electronics have attracted much interest due to the potential of storing vast amounts of information in very small volumes.³

Dipyrromethenes (dipyrins) are monoanionic divalent ligands that form neutral complexes with various metal ions in self-assembly processes.⁴ Porphyrins can be considered as cyclic bis-dipyrromethenes, and Wagner and Lindsey have introduced a molecular wire where a porphyrin array is linked to a boron-dipyrromethene complex at one end of the assembly.⁵ In this case, the boron-dipyrromethene acts as an optical input while the porphyrin array plays the role of the transmission element of the molecular photonic device. Similarly, Weiss and his colleagues have designed a self-assembled porphyrin photonic wire which performs a stepwise energy transfer.⁶ In 2006, Maeda *et al.* employed dipyrins as scaffolds to form metal-coordinated dipyrin polymers which exhibited spherical nanoarchitectures.⁷

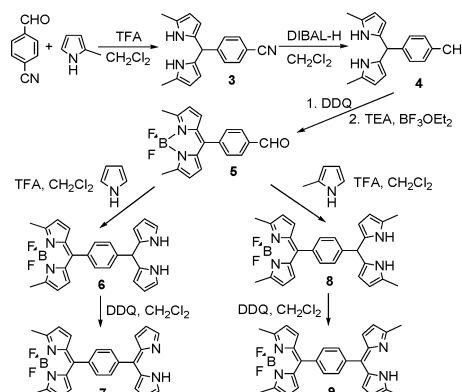
We have prepared a similar dipyrin “dimer” **2** (Scheme 1) but instead of “uncontrolled” polymerization, we have been able to control the oligomerization using a dipyrin dimer monoprotected as the BF₂ complex. Boron-dipyrromethene complexes have properties which combine high molar extinction coefficients and high fluorescence quantum yields, strong chemical and photochemical stabilities in both solution and



Scheme 1

Department of Chemistry, University of British Columbia, 2036 Main Mall, Vancouver, BC, Canada V6T 1Z1.
E-mail: david.dolphin@ubc.ca; Fax: +1-604-822-9678;
Tel: +1-604-822-4571

† Electronic supplementary information (ESI) available: Experimental details; crystal data; ¹H NMR, ¹³C NMR and optical spectra. CCDC 684023–684029 and 709603. For ESI and crystallographic data in CIF or other electronic format, see DOI: 10.1039/b820461f



Scheme 2

the solid state, along with remarkable electron-transfer properties^{8,9} which offer many advantages for future studies.

The protected ligands **7** and **9** were prepared as the primary building blocks (Scheme 2) and when reacted with the dipyrin “dimer”, **2**, oligomers of specific chain lengths were prepared.

The crystal structure† of **7** shows C₂ symmetry, where a nitrogen-bound H-atom on the free-base dipyrromethene unit is shared between N2 and N2' (Fig. 1, the shared proton is marked as grey dots). Consequently, the pyrrole interior C–N–C angles exhibit an average angle of 107.5°, which is intermediate between the amino and imino values for this delocalized aromatic system.

As expected, ligands **7** and **9** are readily able to form unique metal complexes with various metals (Scheme 3). However, mixed coordination reactions of the mono-protected ligand **9** and dipyrin “dimer” **2** produced a mixture, which contains self-assembled oligomers of different lengths (Scheme 4). The formation of the self-assembled oligomers was confirmed by MALDI-TOF mass spectrometry (Fig. 2). The structures of the mono-metal complex **14** and di-metal complex **16** have been defined by X-ray diffraction analysis (Fig. 3).‡ The two crystals show similar metal–N bond lengths and inter-ligand dihedral angles, and complex **16** contains an inversion center.

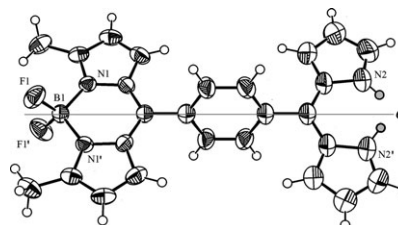
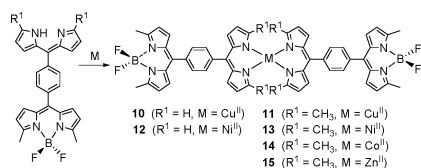
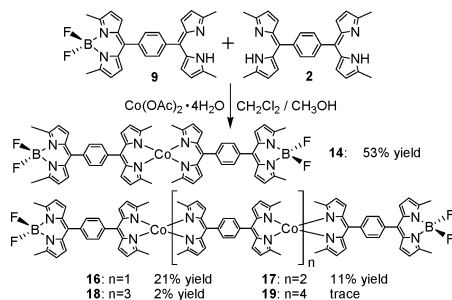


Fig. 1 Crystal structure of **7**. The C₂ symmetry axis is denoted by the gray line. Thermal ellipsoids are scaled to the 50% probability level.



Scheme 3



Scheme 4

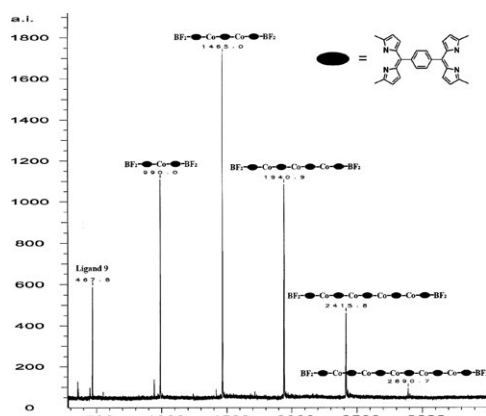


Fig. 2 MALDI-TOF spectrum of the crude reaction mixture which contains an oligomeric mixture of **14**, **16**–**19** and excess ligand **9**.

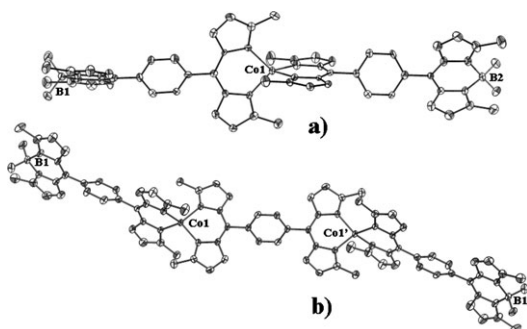


Fig. 3 Crystal structures of **14** (a) and **16** (b); H-atoms have been omitted for clarity. Thermal ellipsoids are scaled to the 50% probability level.

In order to better understand the role of the central metal and the steric effects of the ligand, studies on the crystal structures and spectral properties of various monomeric metal complexes have been undertaken.

All the metal complexes **10**–**15** show nearly linear conformations, in which the two dipyrromethene units linked to the central dicationic metal exhibit distorted tetrahedral structures

Table 1 Selected crystal data

Compound	Inter-ligand dihedral angle/ $^{\circ}$	Bending angle/ $^{\circ}$ ^a	Metal–N bond length/ \AA
10	58.4	20.5	1.92–1.93
11	70.5	8.4	1.95–1.99
12	54.5	19.2	1.89–1.90
13	78.5	2.0	1.96–1.97
14	84.0	3.4	1.96–1.98
15	84.7	3.4	1.97–1.98

^a Bending angle (θ) as shown in Fig. 4.

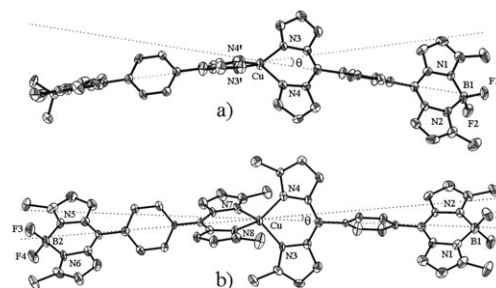
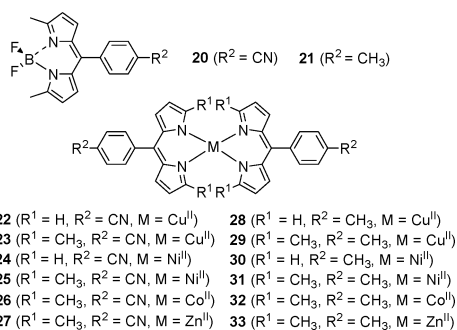


Fig. 4 Crystal structures of **10** and **11** (a and b); H-atoms have been omitted for clarity. Thermal ellipsoids are scaled to the 50% probability level. The bending angle is shown as θ .

as shown by the different dihedral angles of the inter-ligand planes (Table 1). The structures of complexes **10** and **12** show C_2 symmetry, while the others, **11**, **13**–**15**, are non-symmetric molecules (Fig. 4) (see ESI[†]). Interestingly, the two single ligand units of **10** and **12** are bent with 20.5° and 19.2° angles, as shown in Fig. 4. Compared with other metal complexes having the same ligand unit **9**, the Cu^{II} complex **11** shows significant differences in metal–N bond lengths, resulting from the Jahn–Teller effect. Because of steric hindrance between the α -methyl groups, the dihedral angles of metal complexes of **9** were larger than those of the metal complexes of **7**, which are represented by the different coordination geometries and electron distributions in the two Ni^{II} complexes **12** and **13**. The relatively shorter N–Ni bond lengths in complex **12** (1.89–1.90 \AA), compared with those in complex **13** (1.96–1.97 \AA), were considered as the effect of the lower steric hindrance owing to the absence of α -substituents and the reduced radius of the d^8 low-spin state central metal ion. The difference in the coordination and electron distribution is further confirmed by NMR spectroscopy. Complex **12**, having a smaller dihedral angle, showed sharp signals in its 1H NMR spectrum, which proves it is a low-spin, diamagnetic structure. On the other hand, the 1H NMR spectrum of **13** exhibited broad signals over a large range, correlating with a high-spin, paramagnetic structure (see ESI[†]).

While the optical spectra, especially fluorescence, have been thoroughly studied for the boron complexes of dipyrromethenes,^{8,9} those of simple dipyrromethenes and their metal complexes have not been extensively studied. A. I. V'yugin *et al.*¹⁰ examined solvent effects and showed that λ_{max} is determined by the polarization of the π system, which in turn is governed by electronic and steric factors of the metal ions. We have reported¹¹ that hyperconjugation of peripheral alkyl



Scheme 5

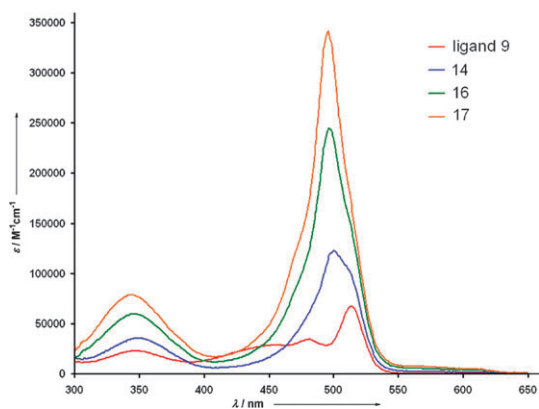


Fig. 5 Optical spectra of ligand **9** and complexes **14**, **16** and **17** in CH_2Cl_2 .

groups results in bathochromic shifts and Motekaitis–Martell MO theory allows for the calculation of dihedral angles for metal complexes.

In this study we have prepared two sets of reference compounds (**20** and **21**, and **22–33**, Scheme 5) to provide the electronic spectra of individual metal-dipyrriins and boron-dipyrriins. For the same metal, an increase in the inter-ligand dihedral angles results in a bathochromic shift (compare **22**, **23**; **28**, **29**; **24**, **25** and **30**, **31**, see ESI[†]). The bathochromic shift also occurs with a cyano group on the *meso*-aryl instead of a methyl group. This is particularly obvious in Ni^{II} complexes where the distorted square-planar structures exhibit a large bathochromic shift (14 nm, compare **24** with **30**). By contrast, the two distorted tetrahedral Ni^{II} complexes of α -methyl dipyrromethenes (compare **25** with **31**) show only a relatively small bathochromic shift (2 nm).

The strongest UV-Vis absorption of ligand **9**, in CH_2Cl_2 , exhibits a sharp band at 514 nm as a result of boron complexation, but this band remains only as a shoulder upon metallation (Fig. 5). The electronic absorption spectra of complexes **14**, **16** and **17** show a hypsochromic shift with increasing length and increasing number of metal ions.

The optical spectra of all the metal complexes **10–17** approximate the sum of the individual boron-dipyrriins and metal-dipyrriins, which suggests a minimal overlap between the π -systems (see ESI[†]).

Dipyrriins allow for great flexibility in the constitution and conformation of the linking groups (and their substitution patterns), peripheral constituents, terminal substituents and

metal coordination. Each of these factors affect step-wise self-assembly into similar arrays and related research is currently in progress.

This work was supported by the Natural Sciences and Engineering Research Council (NSERC) of Canada. We thank the Mass Spectroscopy lab of the Department of Chemistry, University of British Columbia.

Notes and references

† Crystal data for **7**: $\text{C}_{26}\text{H}_{21}\text{BN}_4\text{F}_2$, $M = 438.28$, monoclinic, $a = 6.2217(8)$, $b = 30.104(4)$, $c = 11.954(2)$ Å, $\beta = 96.072(9)^\circ$, $V = 2226.4(6)$ Å³, $T = 298$ K, space group $C2/c$ (no. 15), $Z = 4$, 11946 reflections measured, 2611 unique ($R_{\text{int}} = 0.037$). $R1 = 0.044(I > 2.00\sigma(I))$, $wR2 = 0.122(\text{all data})$. Crystal data for **10**: $\text{C}_{52}\text{H}_{40}\text{B}_2\text{N}_8\text{F}_4\text{Cu}\cdot 2\text{CH}_2\text{Cl}_2$, $M = 1107.93$, orthorhombic, $a = 22.128(5)$, $b = 8.569(2)$, $c = 27.299(6)$ Å, $V = 5176(2)$ Å³, $T = 173$ K, space group $Pbcn$ (no. 60), $Z = 4$, 14088 reflections measured, 3365 unique ($R_{\text{int}} = 0.122$). $R1 = 0.054(I > 2.00\sigma(I))$, $wR2 = 0.136(\text{all data})$. Crystal data for **11**: $\text{C}_{56}\text{H}_{48}\text{B}_2\text{N}_8\text{F}_4\text{Cu}\cdot 2\text{CH}_2\text{Cl}_2$, $M = 1164.04$, monoclinic, $a = 18.142(2)$, $b = 20.146(3)$, $c = 15.483(3)$ Å, $\beta = 90.191(7)^\circ$, $V = 5659(2)$ Å³, $T = 173$ K, space group $P2_1/c$ (no. 14), $Z = 4$, 32007 reflections measured, 7184 unique ($R_{\text{int}} = 0.130$). $R1 = 0.070(I > 2.00\sigma(I))$, $wR2 = 0.209(\text{all data})$. Crystal data for **12**: $\text{C}_{52}\text{H}_{40}\text{B}_2\text{N}_8\text{F}_4\text{Ni}\cdot 2\text{CH}_2\text{Cl}_2$, $M = 1103.10$, orthorhombic, $a = 22.249(2)$, $b = 8.5705(7)$, $c = 27.197(2)$ Å, $V = 5186.1(7)$ Å³, $T = 173$ K, space group $Pbcn$ (no. 60), $Z = 4$, 15765 reflections measured, 3328 unique ($R_{\text{int}} = 0.083$). $R1 = 0.072(I > 2.00\sigma(I))$, $wR2 = 0.121(\text{all data})$. Crystal data for **13**: $\text{C}_{56}\text{H}_{48}\text{B}_2\text{N}_8\text{F}_4\text{Ni}\cdot 2\text{CHCl}_3$, $M = 1228.09$, triclinic, $a = 10.840(1)$, $b = 14.501(2)$, $c = 19.830(2)$ Å, $\alpha = 109.761(6)^\circ$, $\beta = 104.839(6)^\circ$, $\gamma = 93.027(6)^\circ$, $V = 2802.2(5)$ Å³, $T = 173$ K, space group $P\bar{1}$ (no. 2), $Z = 2$, 30194 reflections measured, 9772 unique ($R_{\text{int}} = 0.045$). $R1 = 0.075(I > 2.00\sigma(I))$, $wR2 = 0.230(\text{all data})$. Crystal data for **14**: $\text{C}_{56}\text{H}_{48}\text{B}_2\text{N}_8\text{F}_4\text{Co}\cdot 2\text{CH}_2\text{Cl}_2$, $M = 1159.43$, triclinic, $a = 10.669(1)$, $b = 14.432(2)$, $c = 19.145(2)$ Å, $\alpha = 70.375(4)^\circ$, $\beta = 78.215(4)^\circ$, $\gamma = 86.892(4)^\circ$, $V = 2717.8(5)$ Å³, $T = 173$ K, space group $P\bar{1}$ (no. 2), $Z = 2$, 58453 reflections measured, 10121 unique ($R_{\text{int}} = 0.062$). $R1 = 0.061(I > 2.00\sigma(I))$, $wR2 = 0.169(\text{all data})$. Crystal data for **15**: $\text{C}_{56}\text{H}_{48}\text{B}_2\text{N}_8\text{F}_4\text{Zn}\cdot 2\text{CH}_2\text{Cl}_2$, $M = 1165.87$, triclinic, $a = 10.7063(11)$, $b = 14.4785(12)$, $c = 19.1263(18)$ Å, $\alpha = 70.425(4)^\circ$, $\beta = 78.184(4)^\circ$, $\gamma = 86.994(4)^\circ$, $V = 6037(3)$ Å³, $T = 173$ K, space group $P\bar{1}$ (no. 2), $Z = 2$, 21133 reflections measured, 18068 unique ($R_{\text{int}} = 0.046$). $R1 = 0.066(I > 2.00\sigma(I))$, $wR2 = 0.175(\text{all data})$. Crystal data for **16**: $\text{C}_{84}\text{H}_{72}\text{B}_2\text{N}_{12}\text{F}_4\text{Co}_2\cdot 2\text{CHCl}_3$, $M = 1703.75$, monoclinic, $a = 13.4104(15)$, $b = 26.078(2)$, $c = 12.7437(14)$ Å, $\beta = 115.666(5)^\circ$, $V = 4017.0(7)$ Å³, $T = 173$ K, space group $P2_1/c$ (no. 14), $Z = 2$, 30263 reflections measured, 7078 unique ($R_{\text{int}} = 0.054$). $R1 = 0.059(I > 2.00\sigma(I))$, $wR2 = 0.173(\text{all data})$. CCDC 684023–684029 and 709603. For crystallographic data in CIF or other electronic format, see DOI: 10.1039/b820461f

- J. M. Tour, *Acc. Chem. Res.*, 2000, **33**, 791–804.
- N. Aratani, H. S. Cho, T. K. Ahn, S. Cho, D. Kim, H. Sumi and A. Osuka, *J. Am. Chem. Soc.*, 2003, **125**, 9668–9681.
- J. M. Tour, A. M. Rawlett, M. Kozaki, Y. Yao, R. C. Jagessar, S. M. Dirk, D. W. Price, M. A. Reed, C.-W. Zhou, J. Chen, W. Wang and I. Campbell, *Chem.–Eur. J.*, 2001, **7**, 5118–5134.
- T. E. Wood and A. Thompson, *Chem. Rev.*, 2007, **107**, 1831–1861.
- R. W. Wagner and J. S. Lindsey, *J. Am. Chem. Soc.*, 1994, **116**, 9759–9760.
- M. Koepf, A. Trabolsi, M. Elhabiri, J. A. Wytko, D. Paul, A. M. Albrecht-Gary and J. Weiss, *Org. Lett.*, 2005, **7**, 1279–1282.
- H. Maeda, M. Hasegawa, T. Hashimoto, T. Kakimoto, S. Nishio and T. Nakanishi, *J. Am. Chem. Soc.*, 2006, **128**, 10024–10025.
- M. Wada, S. Ito, H. Uno, T. Murahashima, N. Ono, T. Urano and Y. Urano, *Tetrahedron Lett.*, 2001, **42**, 6711–6713.
- W. Qin, M. Baruah, M. Van der Auweraer, F. C. De Schryver and N. Boens, *J. Phys. Chem. A*, 2005, **109**, 7371–7384.
- G. B. Guseva, E. V. Antina, M. B. Berezin and A. I. V'yugin, *Russ. J. Gen. Chem.*, 2004, **74**, 1282–1285.
- C. Brückner, V. Karunaratne, S. J. Rettig and D. Dolphin, *Can. J. Chem.*, 1996, **74**, 2182–2193.